A Neural Network Approach for Ultrasound Attenuation Coefficient Estimation

Jasleen Birdi[1,2], Jan D'hooge[1] and Alexander Bertrand[2,3]

Email: jasleen.birdi@kuleuven.be, jan.dhooge@kuleuven.be and alexander.bertrand@kuleuven.be

[1]Department of Cardiovascular Sciences, KU Leuven, Leuven, Belgium

[2]Department of Electrical Engineering (ESAT-STADIUS), KU Leuven, Leuven, Belgium

[3]Leuven.AI - KU Leuven Institute for Artificial Intelligence, Leuven, Belgium

Abstract—Quantitative ultrasound (QUS) imaging complements the standard B-mode images with a quantitative representation of the target's acoustic properties. Attenuation coefficient is an important parameter characterizing these properties, with applications in medical diagnosis and tissue characterization. Traditional QUS methods use analytical models to estimate this coefficient from the acquired signal. Propagation effects, such as diffraction, which are difficult to model analytically are usually ignored, affecting their estimation accuracy. To tackle this issue, reference phantom measurements are commonly used. These are, however, time-consuming and may not always be feasible, limiting the existing approaches' practical applicability. To overcome these challenges, we leverage recent advances in the deep learning field and propose a neural network approach which takes the magnitude spectra of the backscattered ultrasound signal at different axial depths as the input and provides the target's attenuation coefficient as the output. For the presented proof-of-concept study, the network was trained on a simulated dataset, and learnt a proper model from the training data, thereby avoiding the need for an analytical model. The trained network was tested on both simulated and tissue-mimicking phantom datasets, demonstrating the capability of neural networks to provide accurate attenuation estimates from diffraction affected recordings without a reference phantom measurement.

Index Terms—quantitative ultrasound, attenuation coefficient, neural network, convolutional layers

I. INTRODUCTION

Acoustic properties of a target tissue play an important role in tissue characterization and diagnostic evaluation of, for instance, kidney [1], breast [2], liver [3], [4], thyroid [5], bone [6], and uterine cervix [7]. The accurate knowledge of these properties is thus relevant for disease detection as well as its progression monitoring. Ultrasound imaging provides a means to extract these properties of interest from the measured ultrasound signal. This is particularly appealing as, unlike other modalities, ultrasound makes use of non-ionizing radiation, is inexpensive and offers portability. Conventionally, ultrasound imaging relies on converting the acquired ultrasound signal from the target tissue to a B-mode image. This, however, provides only qualitative information, discarding the relevant acoustic properties' information present in the signal. The low contrast in these images poses another challenge of acceptable differentiation between different tissues types.

Quantitative ultrasound (QUS) techniques have been developed to counteract these issues, aiming to provide quantitative mapping of these properties on an absolute scale [8], [9]. One of the most relevant acoustic property is the attenuation, characterized by the attenuation coefficient. It has advantages in diagnostic studies, and it is also required for the estimation of other clinically relevant parameters, such as the backscatter coefficient and scatterer size [4], [10]. It thus becomes crucial to design techniques that can provide accurate attenuation coefficient estimates.

Various attenuation coefficient estimation techniques have been proposed in the literature. While some rely on time-domain signals [11]–[13], others work in the spectral domain to extract this coefficient [14]–[19]. The latter set of techniques can broadly be categorised as either relying on spectral analysis of the acquired signal or fitting an analytical physical signal model to the data by a chosen optimization technique. One of the challenges encountered in attenuation coefficient estimation is to compensate for the system-dependent effects that influence the acquired ultrasound backscattered signal, and which are generally difficult to model analytically. If not compensated for, these will cause an inherent mismatch between the acquired signal and the modelled signal, thereby leading to estimation errors. Diffraction is one such prominent effect, which in general is very difficult to correct for in the time domain. In the frequency domain, a common approach to compensate for the system-dependent effects, including diffraction, is to use the available methods in conjuction with reference phantom measurements [14]. It involves taking additional measurements from a reference phantom, whose acoustic properties are known beforehand and comparing it with the signals from a sample. This approach, however, might not be feasible for usage in clinical settings. First, it requires extra measurements from a reference phantom. With change in the adopted ultrasound system settings, these measurements will need to be re-performed. Second, it relies on the assumption that the diffraction effects and the speed of sound in the reference and the sample media are the same, which will not always hold. Another possibility to address this issue is the consideration of plane wave propagation, where the diffraction effects can be neglected. This is limited to specific cases only and might not always be a practical consideration. An ideal and generalized approach to deal with these effects

would be to explicitly model them, which in turn could be integrated in the physical signal model adopted by the existing approaches. Such an analytical formulation, however, does not always exist. Moreover, even for some specific transducer types for which such models exist [20], its integration within the adopted physical signal model induces non-linearity in the overall model, resulting in optimization problems that are difficult to solve with standard solvers.

The existing attenuation coefficient estimation methods, which are inadequate to address the aforementioned issue of diffraction, are primarily based on signal processing and optimization methods to solve the underlying inverse problem. On the other hand, recent years have witnessed a spark interest in the domain of deep learning. It has shown remarkable results in many application areas, often outperforming the respective standard methods in these areas. In particular for ultrasound, major research efforts have been focused on, for instance, improving the image quality [21], classification [22], segmentation [23] and beamforming [24]. The remarkable results obtained highlight the potential of deep learning to capture complex features in ultrasound signals, which otherwise go neglected in traditional approaches. Inspired by this, we take a first step here to implement a deep learning approach for accurate attenuation coefficient estimation. Our proposed approach provides an attenuation coefficient estimate from a given set of backscattered radio-frequency signals, without explicitly modelling the physical signal propagation. The idea is to let the network learn to model the intricacies and complexities of the physical effects encountered during ultrasound wave propagation by providing it with suitable examples. This implicitly helps in avoiding the mismatch between the acquired signal and the modelled signal, inherent in the existing approaches. The proposed approach thus offers a new way to accurately estimate the attenuation coefficient, without being affected by the estimation errors due to the diffraction effects, which are generally not taken into account in analytical models.

The rest of the paper is organized as follows. Section II describes the proposed methodology along with details of the training set considered for the proof of concept in this paper. The experimental details, including the test data specifications and our method's results upon application on these datasets, are presented in Section III. Discussion of the presented work and the concluding remarks are provided in Section IV.

II. METHODS AND MATERIALS

A. Background

In the context of QUS, a region of interest is probed by an acoustic wave transmitted by a transducer. Under certain assumptions, the measured backscattered signal can be modelled in the frequency domain as [14], [16]:

$$|S(f,z)| = |P(f)| \, D(f,z) \, A(f,z) \, B(f,z), \qquad (1)$$

where the different terms are as follows: $|S(f,z)|$ denotes the magnitude spectrum at frequency f of the signal backscattered from depth z, $P(f)$ is the spectrum of the transmitted acoustic wave, $D(f,z)$ incorporates the diffraction effects, $A(f,z)$ denotes the cumulative attenuation of the sample and $B(f,z)$ is the backscatter coefficient. For the case of soft tissues, $A(f,z)$ is typically given by a linear frequency dependence. Considering a homogeneous medium, this translates to $A(f,z) = e^{-2\alpha fz}$, where α is the attenuation coefficient.

The measurements $|S(f,z)|$ are done for a range of frequencies within the usable bandwidth and at different depths within the target. The focus of the current work is then to estimate the attenuation coefficient α given the measured data. This is challenging as all the terms on right hand side of eq. (1) are unknown. In practice, $P(f)$ can be obtained upto a scaling factor by performing a pulse-echo reflector measurement [18]. The other terms still remain unknown. While it is possible to analytically model $B(f,z)$ and estimate it simultaneously with α [16], [18], this is not the case for the diffraction term $D(f,z)$. For an accurate α estimation, the existing methods either neglect these effects or compensate for it by performing additional measurements on a reference phantom, which makes it difficult to use in clinical settings.

B. Proposed approach

To address the aforementioned issues, we propose here a data-driven neural network (NN) approach for attenuation coefficient estimation. Our method relies on a convolutional neural network, making use of the UNet architecture, which is a popular architecture for image segmentation and other applications [25]. The basic architecture used in the current work is illustrated in Fig. 1, where the architecture within the shaded region resembles UNet. The input to the network consists of a 1 dimensional (1D) vector of the concatenated set of backscattered signal's magnitude spectra at different axial depths, which is further described in the next section. It then undergoes a downsampling and an upsampling path, with each path constituted by '1D Conv' layers: performing a 1D convolution followed by the application of a rectified linear unit (ReLU) as the activation function. The kernel weights for the 1D Conv layers are initialized randomly with a normal distribution. In the downsampling path, the two 1D Conv layers (with 4 and 8 filters, respectively, each with a kernel size of 3) are linked to each other via a max pooling operation. For the upsampling path, transposed convolution in combination with concatenation of the corresponding layer in the downsampling path is done. This is then further processed by a 1D Conv layer with 4 filters (kernel size 3), followed by a 1D Conv layer with 1 filter (kernel size 1). In our case, the network is designed to provide the attenuation coefficient as the output, which is a scalar quantity. This attenuation estimate is obtained from a fully connected layer.

A detailed overview of the network specifications is presented in the following.

C. Network & Input data specifications

For this proof-of-concept study, we train our network on simulated datasets, which offers the possibility to generate a large data sample as well as the precise knowledge of the
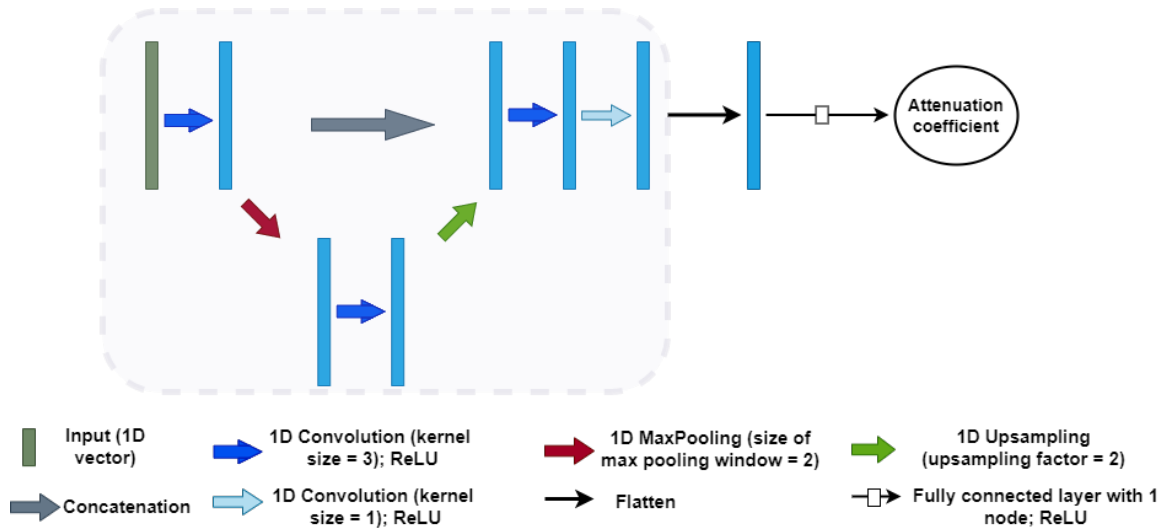
Fig. 1. Illustration of the basic architecture of the proposed neural network approach for attenuation coefficient estimation. It is based on the UNet architecture, with the usage of a fully connected layer at the end to obtain a single attenuation coefficient for each input data. The input data to the network is a 1D vector of the backscattered ultrasound signal's magnitude spectra concatenated at different axial depth points.

ground-truth attenuation coefficient. Moreover, the data needs to be diverse to avoid issues with overfitting and generalization to new data. With this in mind, the data was generated in the Field II simulator [26] using a 3.5 MHz transducer for a 60 mm medium consisting of randomly distributed scatterers. Data with 5 different realizations of the scatterer's random positions were simulated. For the attenuation coefficient α, 20 different values between 0.5 to 2 dB/cm/MHz were considered to train the network on datasets with different attenuation values. Further, for each case, the data was generated using 6 different focal lengths of the transducer to ensure incorporation of a diverse set of diffraction affected spectra in the training data. The generated data consists of the backscattered radio-frequency (RF) lines, which were then converted to the frequency domain to get the magnitude spectrum. This process involves dividing the whole axial depth into multiple windows and computing the magnitude spectrum for each of the windowed signal via a discrete Fourier transform [18]. In the current setting, we considered a window length of 4 mm with 50% overlap and 15 dB usable bandwidth, which resulted into 28 windows and 452 frequency points in each windowed spectrum. Finally, the input to the proposed network was the obtained magnitude spectrum, concatenated over different depths/windows in a 1D vector, for a given RF line.

The data was augmented to include scaled copies as well as different crops of 15 subsequent windows from the total depth of 28 windows (thereby reducing the input dimension of the network). While the former ensures scale-invariance of the trained network, the latter is used to warrant its shift-invariance. This resulted in the input dataset with $\sim 400,000$ samples, with each input vector of size 6780. The dataset was randomly divided in a training, validation and test set, containing 75%, 15% and 10% of the data, respectively.

TABLE I
ACOUSTIC PROPERTIES OF THE TISSUE-MIMICKING PHANTOMS USED FOR THE PROPOSED APPROACH'S TESTING.

	Phantom	Attenuation coefficient (dB/cm/MHz)	speed of sound (m/s)
First set	1,2	0.61	1546
	3	0.63	1552
	4,5	0.84	1520
Second set	6	0.65	1492
	7	0.67	1492

The network has ~ 7000 parameters, trained using Keras[1]. The mean squared error between the network's output and the ground-truth attenuation coefficient value was used as the loss function. The Adam optimizer [27] with learning rate set to 10^{-4} was employed. 50 epochs were considered with a batch size of 100. These hyperparameters (including the network dimensions) were manually and empirically tuned based on performance on the validation set.

III. EXPERIMENTS

A. Test data specifications

The performance of the network was assessed on the simulated data test set, as well as on real ultrasound data recorded from different tissue-mimicking phantoms. The details of the used phantoms can be found in [17], [28]. The measurements were performed in pulse-echo mode with a single transducer acting as both emitter and receiver. Two sets of homogeneous phantoms were considered with their attenuation coefficients given in Table I. For the first set [28], the data was collected
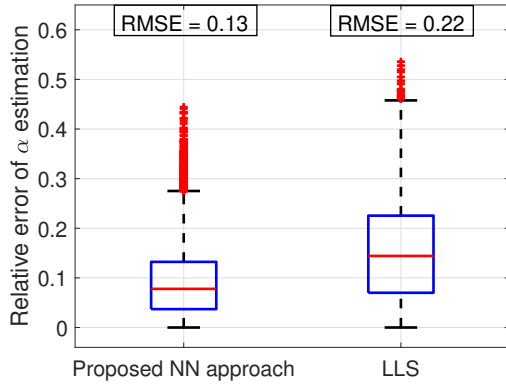
[1]https://keras.io/

Fig. 2. Results on simulated test data showing relative error of attenuation coefficient (α) estimation as obtained by the proposed neural network (NN) approach and the benchmark LLS method. The obtained RMSE value in the two cases is listed at the top of each box plot.

Phantom	Relative error		RMSE	
	Proposed NN approach	LLS	Proposed NN approach	LLS
1	0.23	0.31	0.16	0.19
2	0.11	0.27	0.09	0.17
3	0.06	0.03	0.08	0.02
4	0.15	0.10	0.08	0.04
5	0.12	0.25	0.11	0.16
6	0.40	1.01	0.27	0.71
7	0.24	1.05	0.16	0.70

B. Results

a) Simulated test data: The results obtained by applying the proposed NN approach and the benchmark LLS approach on the simulated test data are depicted as box plots in Fig. 2, indicating the spread of errors over the considered large number of samples. Our approach provided attenuation coefficient estimates with $\sim 6\%$ lower mean relative error and 9% lower RMSE than the LLS estimates.

b) Tissue-mimicking phantom data: Table II illustrates the attenuation coefficient estimation errors (relative error and RMSE) as obtained by the proposed NN approach and the LLS method on the two phantom datasets. In this case, given only 10 data samples per phantom, the relative error averaged over these samples is reported. For the first set, in most of the cases, the NN approach performed better than LLS, with an overall mean error of 15% compared to 19.36% for LLS, computed over all the phantoms.

For the second type of phantom data, the proposed approach provided attenuation coefficient estimates with much lower errors than LLS estimates. For the latter, the estimates were highly inaccurate, with a relative error $> 100\%$.

using three different types of flat unfocused single-element transducers: a V306-SU with center frequency of 2.25 MHz and 60% bandwidth, an A306-SU with center frequency of 2.25 MHz and 50% bandwidth and a V309-SU with center frequency of 5 MHz and 65% bandwidth (Panametrics NDT, Inc., Waltham, MA). The measurements were performed in the far-field of the respective transducers to avoid near-field diffraction effects. Therefore, we expect model-based attenuation estimators to work relatively good, even without a normalization via a reference phantom.

The second phantom dataset is the one from [17], for which the data for the sample phantom was taken along with a reference phantom so as to compensate for the diffraction effects. Within the context of the current work, the measurements for the sample and reference phantom, each one of which is affected by diffraction effects, were used separately. A 9L4 linear array transducer on a Siemens Acuson S3000 (Issaquah, WA) with a center frequency of 6.6 MHz was used to acquire 10 uncorrelated RF data frames. For both phantom datasets, the data was normalized with the respective transducer's impulse response function.

As a benchmark, we use a state-of-the-art model-based attenuation estimator from [18], which casts the analytical model (1) to a linear least squares (LLS) problem. It has been shown to outperform other approaches in the literature, both in terms of accuracy and variance. However, this method works in cases where the diffraction effects are negligible or can be compensated for using reference phantom measurements.

Finally, for the method's performance assessment, we report two metrics. First, for the ith data sample, with $i \in \{1, \dots, N\}$ (N being the total number of data samples in the test set), the relative error between the true attenuation coefficient α_i and the estimated value $\hat{\alpha}_i$ is defined as: Rel err$_i = |\alpha_i - \hat{\alpha}_i|/|\alpha_i|$. Second, the standard metric of root mean square error (RMSE) between the true and the estimated attenuation coefficient was computed as: RMSE $= \sqrt{\frac{\sum_{i=1}^{N}(\alpha_i - \hat{\alpha}_i)^2}{N}}$.

IV. DISCUSSION AND CONCLUSION

We have presented a neural network (NN)-based approach for attenuation coefficient estimation in quantitative ultrasound imaging. Our method is based on a NN architecture that takes the magnitude spectrum of the backscattered ultrasound signal at different axial depths as the input and provides an estimate of the attenuation coefficient of the underlying medium as the output. It benefits from learning the complex physical effects encountered in the signal propagation path, without relying on an explicit analytical model, which might not always exist, e.g., for diffraction effects. We considered different types of datasets, both simulated as well as experimental data from tissue-mimicking phantoms to test the network's performance. While the network was trained only on simulated data, the results showed it performed well even on phantom data. Moreover, the proposed approach performed better than the

benchmark linear least squares (LLS) based method, especially for the case of phantoms largely affected by diffraction effects.

For the first phantom dataset, it can be observed that even in the case when the experiment was performed in the transducer's far-field to diminish the diffraction effects as much as possible, the proposed approach performed better than LLS. Further, for the case with measurements highly influenced by the diffraction effects, we tested our approach without considering the reference phantom measurements to compensate for these effects. Our approach managed to estimate the coefficients with a much lower estimation error than LLS (without compensations via a reference phantom). These findings put forward the current work as a proof-of-concept study, highlighting that the NN approach has the potential to surpass the estimation performance by the existing approaches without requiring an analytical signal model. Inclusion of more diverse data, for instance, with different transducer settings on various tissue-mimicking phantoms, for training the network can potentially lead to even better performance. This is further expected to alleviate the current need of data normalization with the transducer's impulse response function.

The current work considered homogeneous medium settings, both for simulated as well as tissue-mimicking phantom data. In practical scenarios with heterogeneous medium, i.e. spatially varying attenuation coefficient, our approach can be applied on the homogeneous regions-of-interest selected within the heterogeneous medium. Further extension of the approach to a fully automated attenuation mapping of the target heterogeneous medium needs to be investigated and will be explored in future.

ACKNOWLEDGMENT

REFERENCES

[1] M. F. Insana, T. J. Hall, J. G. Wood, and Z. Y. Yan, "Renal ultrasound using parametric imaging techniques to detect changes in microstructure and function," *Investigative radiology*, vol. 28, no. 8, pp. 720–725, 1993.

[2] K. Nam, J. A. Zagzebski, and T. J. Hall, "Quantitative assessment of in vivo breast masses using ultrasound attenuation and backscatter," *Ultrason. Imaging*, vol. 35, no. 2, pp. 146–161, 2013.

[3] N. Maklad, J. Ophir, and V. Balsara, "Attenuation of ultrasound in normal liver and diffuse liver disease in vivo," *Ultrason. Imaging*, vol. 6, no. 2, pp. 117–125, 1984.

[4] R. Kuc, "Clinical application of an ultrasound attenuation coefficient estimation technique for liver pathology characterization," *IEEE Trans. Biomed Eng*, no. 6, pp. 312–319, 1980.

[5] Y. Fujii, N. Taniguchi, K. Itoh, and K. Omoto, "Attenuation coefficient measurement in the thyroid," *J. ultrasound med*, vol. 22, no. 10, pp. 1067–1073, 2003.

[6] C. Langton, S. Palmer, and R. Porter, "The measurement of broadband ultrasonic attenuation in cancellous bone," *Eng Med*, vol. 13, no. 2, pp. 89–91, 1984.

[7] B. L. McFarlin, V. Kumar, T. A. Bigelow, D. G. Simpson, R. C. White-Traut, J. S. Abramowicz, and W. D. O'Brien Jr, "Beyond cervical length: A pilot study of ultrasonic attenuation for early detection of preterm birth risk," *Ultrasound Med. Biol.*, vol. 41, no. 11, pp. 3023–3029, 2015.

[8] F. L. Lizzi, M. Greenebaum, E. J. Feleppa, M. Elbaum, and D. J. Coleman, "Theoretical framework for spectrum analysis in ultrasonic tissue characterization," *J. Acoust. Soc. America*, vol. 73, no. 4, pp. 1366–1373, 1983.

[9] J. Mamou and M. L. Oelze, *Quantitative ultrasound in soft tissues*. Springer, 2013.

[10] T. A. Bigelow and W. D. O'Brien Jr, "Scatterer size estimation in pulse-echo ultrasound using focused sources: Calibration measurements and phantom experiments," *The Journal of the Acoustical Society of America*, vol. 116, no. 1, pp. 594–602, 2004.

[11] P. He and J. Greenleaf, "Attenuation estimation on phantoms—a stability test," *Ultrasonic imaging*, vol. 8, no. 1, pp. 1–10, 1986.

[12] H. S. Jang, T. K. Song, and S. B. Park, "Ultrasound attenuation estimation in soft tissue using the entropy difference of pulsed echoes between two adjacent envelope segments," *Ultrasonic imaging*, vol. 10, no. 4, pp. 248–264, 1988.

[13] B. Knipp, J. Zagzebski, T. Wilson, F. Dong, and E. Madsen, "Attenuation and backscatter estimation using video signal analysis applied to b-mode images," *Ultrasonic Imaging*, vol. 19, no. 3, pp. 221–233, 1997.

[14] L. X. Yao, J. A. Zagzebski, and E. L. Madsen, "Backscatter coefficient measurements using a reference phantom to extract depth-dependent instrumentation factors," *Ultrason. Imaging*, vol. 12, no. 1, pp. 58–70, 1990.

[15] R. Kuc and M. Schwartz, "Estimating the acoustic attenuation coefficient slope for liver from reflected ultrasound signals," *IEEE Trans. Sonics Ultrason.*, vol. 26, no. 5, pp. 353–361, 1979.

[16] K. Nam, J. A. Zagzebski, and T. J. Hall, "Simultaneous backscatter and attenuation estimation using a least squares method with constraints," *Ultrasound Med. Biol.*, vol. 37, no. 12, pp. 2096–2104, 2011.

[17] N. Jafarpisheh, T. J. Hall, H. Rivaz, and I. M. Rosado-Mendez, "Analytic global regularized backscatter quantitative ultrasound," *IEEE Trans. Ultrason., Ferroelectr., Freq. Control*, vol. 68, no. 5, pp. 1605–1617, 2020.

[18] J. Birdi, A. Muraleedharan, J. D'hooge, and A. Bertrand, "Fast linear least-squares method for ultrasound attenuation and backscatter estimation," *Ultrasonics*, p. 106503, 2021.

[19] J. Birdi, J. D'hooge, and A. Bertrand, "Spatially variant ultrasound attenuation mapping using a regularized linear least-squares approach," *IEEE Trans. Ultrason., Ferroelectr., Freq. Control*, vol. 69, no. 5, pp. 1596–1609, 2022.

[20] X. Chen, D. Phillips, K. Q. Schwarz, J. G. Mottley, and K. J. Parker, "The measurement of backscatter coefficient from a broadband pulse-echo system: A new formulation," *IEEE transactions on ultrasonics, ferroelectrics, and frequency control*, vol. 44, no. 2, pp. 515–525, 1997.

[21] S. Vedula, O. Senouf, A. M. Bronstein, O. V. Michailovich, and M. Zibulevsky, "Towards ct-quality ultrasound imaging using deep learning," *arXiv preprint arXiv:1710.06304*, 2017.

[22] H. Ravishankar, P. Sudhakar, R. Venkataramani, S. Thiruvenkadam, P. Annangi, N. Babu, and V. Vaidya, "Understanding the mechanisms of deep transfer learning for medical images," in *Deep learning and data labeling for medical applications*. Springer, 2016, pp. 188–196.

[23] Y. Xu, Y. Wang, J. Yuan, Q. Cheng, X. Wang, and P. L. Carson, "Medical breast ultrasound image segmentation by machine learning," *Ultrasonics*, vol. 91, pp. 1–9, 2019.

[24] A. C. Luchies and B. C. Byram, "Deep neural networks for ultrasound beamforming," *IEEE transactions on medical imaging*, vol. 37, no. 9, pp. 2010–2021, 2018.

[25] O. Ronneberger, P. Fischer, and T. Brox, "U-net: Convolutional networks for biomedical image segmentation," in *International Conference on Medical image computing and computer-assisted intervention*. Springer, 2015, pp. 234–241.

[26] J. A. Jensen, "Simulation of advanced ultrasound systems using field ii," in *2004 2nd IEEE International Symposium on Biomedical Imaging: Nano to Macro (IEEE Cat No. 04EX821)*. IEEE, 2004, pp. 636–639.

[27] D. P. Kingma and J. Ba, "Adam: A method for stochastic optimization," *arXiv preprint arXiv:1412.6980*, 2014.

[28] N. Ilyina, J. Hermans, E. Verboven, K. Van Den Abeele, E. D'agostino, and J. D'hooge, "Attenuation estimation by repeatedly solving the forward scattering problem," *Ultrasonics*, vol. 84, pp. 201–209, 2018.